International Journal of Heat and Mass Transfer 78 (2014) 852–859

Contents lists available at ScienceDirect

International Journal of Heat and Mass Transfer

journal homepage: www.elsevier.com/locate/ijhmt

Self-induced Marangoni flow in evaporating alcoholic solutions

Anselmo Cecere [a,*], Cosimo Buffone [b], Raffaele Savino [a]

[a] Dipartimento di Ingegneria Industriale (DII) – Sezione Aerospaziale, Università degli Studi di Napoli Federico II, Piazzale Tecchio, 80, 80125 Napoli, Italy
[b] Microgravity Research Centre, Université libre de Bruxelles, Avenue F. Roosevelt 50, 1050 Bruxelles, Belgium

ARTICLE INFO

Article history:
Received 2 March 2014
Received in revised form 19 July 2014
Accepted 20 July 2014

Keywords:
Marangoni flow
Micro-channel
Meniscus
Binary mixtures
Evaporation

ABSTRACT

The self-induced Marangoni convection in alcoholic solutions is the subject of the present experimental investigation. Pure ethanol and its mixtures with 5%, 10% and 20% in weight of water are presented and discussed. In particular, Marangoni flow in horizontal pipes from 100 to 1000 μm inner diameter is studied. Vortex spinning frequency, average particle tracers velocity and evaporation rate are measured and discussed. The evaporation rate increases and the evaporation flux decreases at bigger tube sizes in line with previous investigations; pure ethanol has higher evaporation rate and flux than ethanol/water mixtures. The spinning frequency and the average tracer particles velocity decrease for increasing water content in the mixtures. All of these findings are due to evaporative cooling effect which is higher at the meniscus wedge (where the triple-line region is found) than at the meniscus center; this causes a difference in temperature between the wedge and the center that generates a gradient of surface tension driving vigorous Marangoni convection, that has been reported and analyzed. The experimental results are explained on the basis of a numerical model including evaporation, vapor diffusion, heat and mass transfer from the liquid to the surrounding ambient and the Marangoni effects.

1. Introduction

Many industrial applications such as combustion, spreading of drops, evaporation and condensation of liquid films rely on thermocapillary phenomena. Usually, thermocapillary flow is important in applications with temperature gradients on free surfaces such as crystal growth [1], welding and glass manufacture [2]. Recent extensions of these studies find applications to problems encountered in micro-electro-mechanical devices, or for the development of more efficient heat transfer and thermal control systems, micro heat pipes, micro fluidic systems. An overview of different scientific developments on the subject, with particular attention to potential technological applications, is presented in Ref. [3].

Phenomena arising from interfacial tension gradients have been initially discovered in the frame of chemical engineering processes, where fluid flows arising from surface composition differences play a major role. Solutal Marangoni instabilities typically arise in systems involving mass transfer of surface-active compounds. However, there are many other situations where interface tension-driven effects have practical importance, for instance convective flows induced in non-uniformly heated liquids by surface tension variations induced by temperature gradients (sometimes addressed as thermocapillary convection). In the 1950s Pearson [4] investigated a liquid layer heated from below and attributed the observed convection pattern to surface tension; he also introduced for the first time the Marangoni number.

Unfortunately, in most circumstances under normal gravity conditions on Earth, Marangoni effects are masked by natural convection induced by density differences. For this reason, surface tension effects within liquids have attracted the attention of several scientists in microgravity experiments on space laboratories. On the other hand, the role of surface tension becomes dominant decreasing the Bo number, i.e. decreasing the system size and or in microgravity conditions. This is the case of evaporating drops or menisci commonly used in a number of heat transfer devices like heat pipes and micro-channels using porous wicks and grooved structures [5].

Kavehpour et al. [6] have shown that the evaporation of silicon oil drop can lead to interfacial temperature gradients that generate thermocapillary stresses. Zhang and Chao [7] attributed the convective patterns in an evaporative liquid layer to the cooling of the interface because of the higher evaporation rates. Pratt and Hallinan [8] and Pratt et al. [9] investigated the stability of pentane inside a vertically oriented capillary tube with the meniscus positioned below a heater. They observed that thermocapillary stresses arising from temperature gradients are responsible for meniscus recession down the capillary tube. The authors did not investigate the hydrodynamics of the flow in the meniscus liquid phase.

* Corresponding author. Tel.: +39 081 768 23 58.
E-mail address: anselmocecere@hotmail.com (A. Cecere).

http://dx.doi.org/10.1016/j.ijheatmasstransfer.2014.07.055
0017-9310/

Nomenclature

x	liquid mole fraction
y	liquid vapor fraction
c	concentration
D	ethanol/air diffusion coefficient
D_L	ethanol/water diffusion coefficient
h	heat transfer coefficient
H_{LV}	latent heat of vaporization
ID	inner diameter
J	evaporative mass flux
P	pressure
P_s	saturated vapor pressure
$\dot{q}$	heat flux
S	surface coordinate
T	temperature
V	velocities

Greek symbol

ρ	density
μ	viscosity
α	thermal diffusivity
σ_T	surface tension derivative
τ	viscous shear stress

Subscripts

L	liquid
V	vapor
S	satured

Evaporation in capillary tubes has been also the subject of a number of publications by one of the present authors. Evaporation rate and fluxes on a single receding and double menisci (one of which pinned at the capillary tube mouth) has been reported in Buffone and Sefiane [10] for different tube sizes and alcohols; the authors also reported the vortex cross section frequency with some maps of μ-Particle Image Velocimetry (μ-PIV). The authors conclude that the non-uniform evaporation at the meniscus interface is responsible for a strong convection in the liquid phase driven by surface tension gradient. The mass flux and the vortex frequency are found to be higher for smaller tube sizes.

In Buffone and Sefiane [11] the authors measure the temperature profile along the meniscus interface at the tube mouth and on the side of the tube. The measurements have been performed for different alcohols and tube sizes and clearly show the sink effect at the meniscus triple line due to the peak of evaporation in that region. Buffone et al. [12] reported the important distortion of the toroidal Marangoni convection vortex inside capillary tubes horizontally positioned for methanol and ethanol; they found by the use of μ-PIV that the horizontal cross sections of the vortex cells are symmetrical with respect to the tube axis, whereas the vertical cross section is asymmetrical. Dhavaleswarapu et al. [13] reproduced the results of Buffone and Sefiane [10] and Buffone et al. [12] by analyzing five different tube sizes ranging from 75 to 1575 μm using μ-PIV. They found that the evaporation rate and flux scale parabolically and hyperbolically respectively instead of linearly as in Buffone and Sefiane [10]; the vorticity scales hyperbolically with the tube diameter in contrast with the linear relationship of Buffone et al. [12]. Dhavaleswarapu et al. [13] argue that Buffone and Sefiane [11] and Buffone et al. [12] used only three tube sizes for their experiments.

Chamarthy et al. [14] reported μ-PIV measurements of horizontally oriented capillary tubes with ethanol as working fluid; in particular they looked at different horizontal cross sections of the tube and also at the vertical cross section. They found distortion of the flow field which they attributed to the action gravity; interestingly they reported that there is no distortion of the flow pattern for capillary sizes of 75 μm. This is a very interesting finding with important repercussions in industrial and laboratory applications such as crystal growth. Instabilities of the toroidal Marangoni vortex have been reported in Pan et al. [15]; the authors positioned an evaporating meniscus of ethanol in a 625 μm cylindrical channel. They show that the Marangoni flow in a concave meniscus is always symmetrical to the tube axis whereas that on a convex meniscus loses symmetry with only one vortex occupying the whole channel. Additionally, it was shown that the inwards (from the meniscus wedge to its center) Marangoni flow is found not as stable as the outwards flow. They also found that for the inward flow to lose symmetry the bulk fluid must be warmer than the meniscus and the Marangoni number must be above a specified value.

Instabilities on the Marangoni flow, the meniscus position and its temperature were reported in Buffone et al. [16] for ethanol in a 900 μm cylindrical horizontal channel. The authors developed a linear stability analysis and attributed the instabilities to the competition of gravity and surface tension forces. Marangoni oscillatory periodic instabilities in a 1 mm square glass tube filled with ethanol have also been recently reported in Minetti and Buffone [17], where digital holographic microscopy has been used to trace a seeding particle in its three-dimensional trajectory.

In the present work Marangoni flows induced by the self-evaporation in horizontal capillary tubes have been studied considering binary mixtures. Pure ethanol and ethanol/water mixtures of different concentrations have been investigated using capillary tubes of 100, 200, 400, 600, 800 and 1000 μm internal diameters. Works on Marangoni convection in binary mixtures are rare as also reported by Zhang et al. [18]. The authors work with liquid films of NaCl and water in open air; they find that evaporation is important to the flow pattern at the beginning whereas the Soret effect becomes significant at later stages. For the present experimental investigation, to the authors' knowledge it is the first time that such study inside capillaries tubes has been carried out. The Marangoni convection is characterized by measuring the evaporation rate, the Marangoni vortex spinning frequency and the velocities in the liquid. The reported Marangoni convection is self-induced because of the differential evaporation rate along the curved meniscus interface. Analyses of the experimental results are given under the assumption of diffusion limited evaporation process in the vapor phase. Marangoni convection and particle trajectories have been reconstructed numerically using a computational fluid dynamic model.

2. Experimental setup

Capillary tubes of borosilicate glass with ID of 100, 200, 400, 600, 800, and 1000 μm with a total length of 100 mm have been used. The tubes are used as received from the manufacturer (Vitro-Com). For all flow characterization the experimental apparatus consists of a microscope, a CCD camera with 752 × 480 pixels, nylon tracer particles with average diameter of 15 μm, and a computer with "home-made" software (Fig. 1).

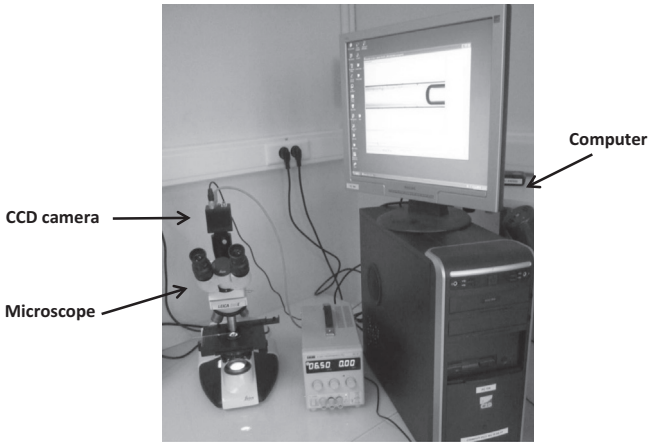

Fig. 1. Experimental apparatus for flow visualization. Marangoni flow in microchannel is observed using a microscope equipped with a CCD camera.

Pure ethanol and its mixtures with water have been analyzed. In particular, 5%, 10% and 20% in weight of water in ethanol are considered. The tubes are partially filled (between 30% and 40% of the total length) with the working fluid from one end and then by tilting the tube one meniscus is pinned at the tube mouth where evaporation takes place, while the other meniscus recedes inside the tube to account for mass lost (Fig. 2a). As reported by Buffone and Sefiane [11], the majority of the evaporation takes place at the meniscus pinned at the tube mouth while for the second meniscus it is too far from the opposite tube end and therefore vapor would have to diffuse for such long distance that in practice there is no appreciable evaporation at this latter meniscus. The evaporation is a spontaneous process and happens in open air and is due to the vapor pressure of the working fluid being lower that its partial pressure in air. The capillary tubes are positioned horizontally and only diametrical horizontal sections of the tubes have been done as in Buffone and Sefiane [11]. Fig. 2b is a superimposition of 20 frames and shows the trajectories of tracer particles near the meniscus interface at the tube mouth; it is evident the presence of two counter rotating vortices symmetrical with respect to the tube axis.

The evaporation rate at the meniscus pinned at the tube mouth can be measured by following the receding meniscus inside the tube as done also in Buffone and Sefiane [11] (Fig. 2a) for pure liquids. In case of binary mixtures, alcohols evaporate faster than water. It is assumed that the evaporation of water is negligible and the evaporation rate is mainly due to the evaporation of ethanol, which is the richer component in the mixtures. For the evaporation rate measurements all the six tube sizes have been considered. The spinning frequency is measured by following a tracer particle while it makes a revolution in the Marangoni vortex. The average particle speeds are characterized by measuring the vortex horizontal sections in a loop. For these measurements only tube sizes 400, 600, 800 and 1000 μm have been considered.

In order to reconstruct the spinning frequency a model based on Discrete Phase Model has been used to simulate particle motion inside the capillary tube. Fig. 2c shows the particle trajectory eval-

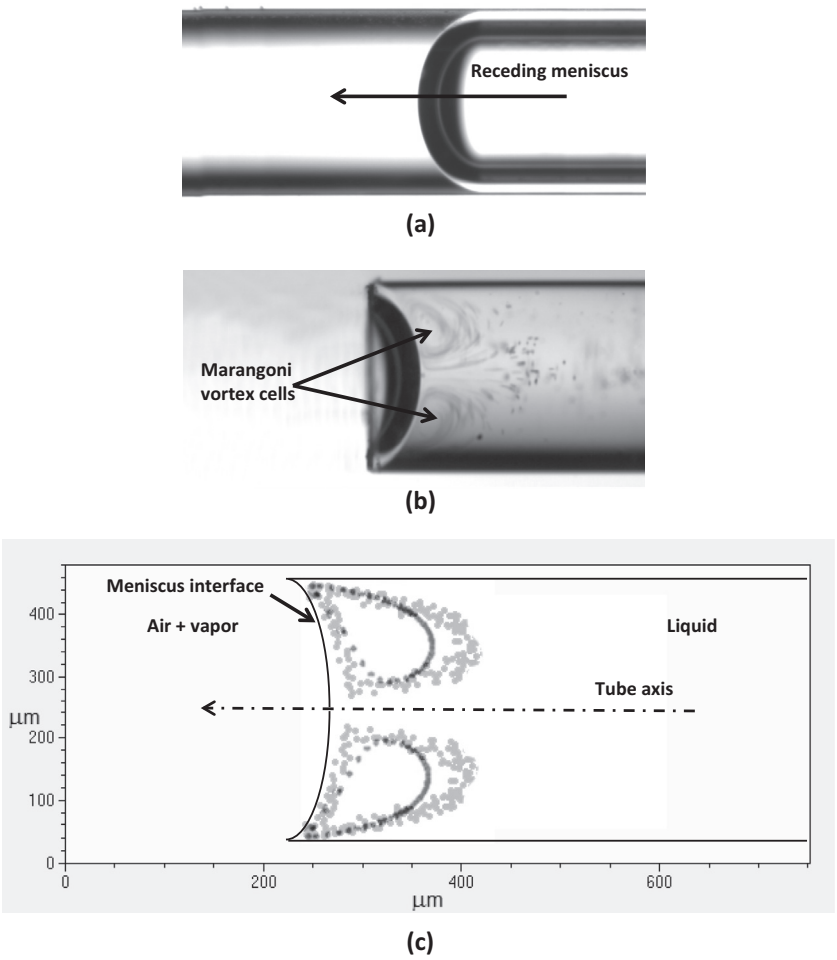

Fig. 2. Typical experimental results. (a) Image of the receding meniscus. (b) Superposition of 20 images of tracers particles unveiling two optical sections of the Marangoni toroidal vortex. (c) Tracer particles trajectory for the two Marangoni vortex optical sections (gray color) with superimposed numerical results (black color).

uated numerically superimposed to the convective cells obtained experimentally.

3. Experimental results and discussion

The results to be reported and discussed in this work refer to the self-induced Marangoni convection due to the non-uniform evaporation in still air along a curved meniscus interface pinned at the tube mouth. The evaporation along the curved meniscus interface is higher at the meniscus wedge than in the center. This leads to an evaporative cooling effect and a consequent lower temperature at the meniscus wedge than at the center. This mechanism has been reported and explained in detail in many previous publications (Buffone and Sefiane [10,11], Buffone et al. [12], Dhavaleswarapu et al. [13] and Chamarthy et al. [14]). In a different publication Wang et al. [19] postulate explanation related to the diffusion of vapor in the air/vapor phase above the meniscus; they argue that the evaporation rate is higher at the meniscus wedge than at the center because the wedge is closer to the tube mouth than the center and therefore the vapor diffuses more easily at the wedge.

The first results reported are those of the evaporation rate and mass flux for ethanol–water binary mixtures. Fig. 3 reports on the right vertical axis the evaporation rate and on the left one the mass flux.

Evaporation rate was evaluated neglecting the shape of the meniscus and taking into account the tube diameter. As shown by Fig. 3, the evaporation rate is a monotonically increasing function of the tube diameter and the mass flux a nearly hyperbolic function of the tube diameter. In addition, the evaporation rate and mass flux are higher for pure ethanol and decrease with increasing content of a much less volatile liquid which is water. The differential evaporation of the two components for binary solutions changes the concentration of the alcohols in the mixtures. Let us assume that the there is no evaporation of water. Considering the worst case of 1 mm tube diameter, which shows the higher evaporation rate, and taking into account the typical acquisition time needed for the measurements (5 min) the mass loss of the alcohol for mixtures at 5% and 20% is 0.2% and 0.4%, respectively. This gives a concentration variation that is assumed to be negligible. Similar conclusions can be obtained for the spinning frequency measurements where the acquisition time is much less (30 s).

The evaporation rate and flux are a function of the tube diameter because most of the evaporation takes place at the meniscus micro-region which scales almost linearly with the tube size as also reported in Dhavaleswarapu et al. [13]. Higher contents of water reduce the evaporation rate and flux because there is less concentration of the more volatile component (ethanol) at the meniscus triple line region.

The spinning frequency and the average speed of the tracer particles are plotted in Fig. 4 for a selection of the tube sizes and for increasing water concentration. Fig. 4a shows that the spinning frequency is a monotonically decreasing function of the tube size and higher concentrations of water result in reduced spinning frequencies. This behavior is in agreement with the results reported in Dhavaleswarapu et al. [13]. The average tracer particle speed as the tracer completes a loop of the Marangoni roll, evaluated by the simple equation $V = lf$ where l is the overall length of loop and f is the spinning frequency, is reproduced in Fig. 4b for all liquids. The average tracer speed decreases at larger tube sizes and for higher water concentrations. This is due to the fact that the driving force of the Marangoni convection is lower for increased tube sizes and at increasing the water concentration.

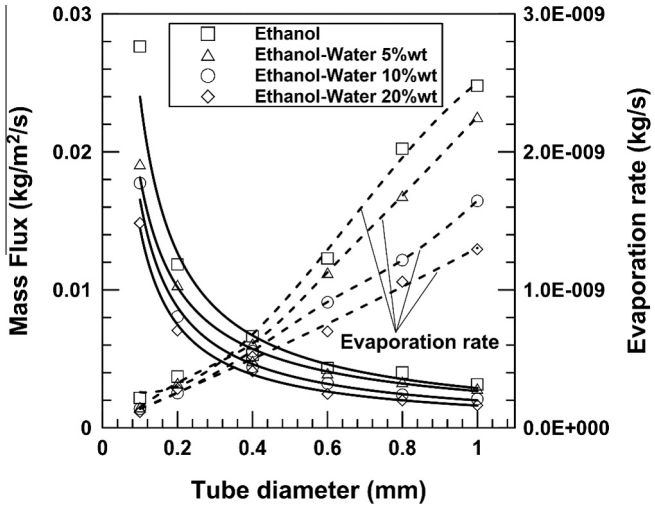

Fig. 3. Evaporation rate (increasing functions) and average mass flux (decreasing functions) versus tube diameter, for ethanol–water mixtures.

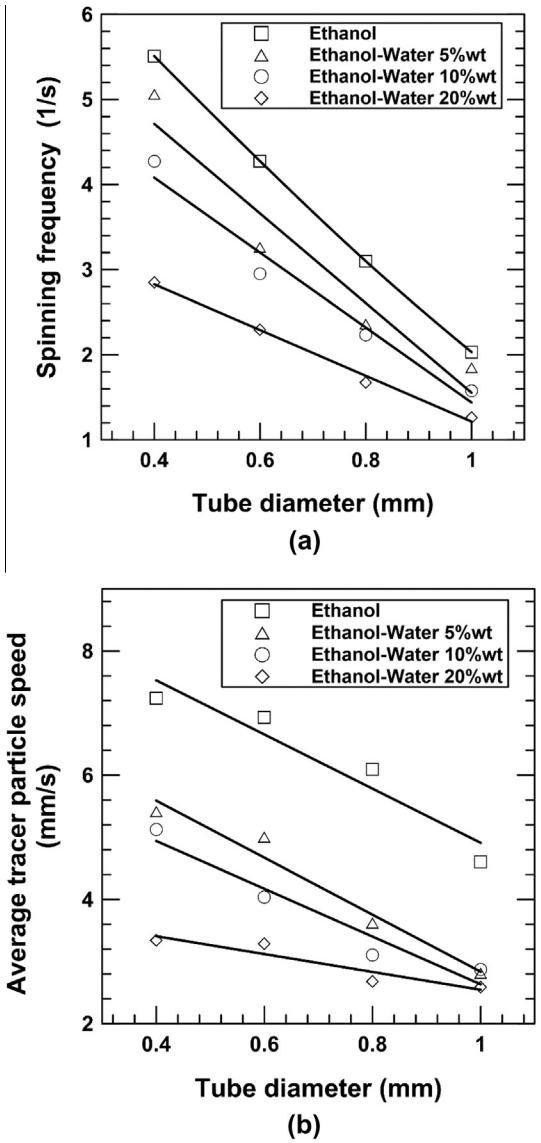

Fig. 4. (a) Spinning frequency of the Marangoni vortex as a function of tube diameter for ethanol–water mixtures. (b) Average tracer particle speed over an entire loop of the Marangoni vortex as a function of tube diameter for ethanol–water mixtures.

4. Numerical model

For the evaporation problem considered in the present study the Knudsen number, a dimensionless parameter defined as the ratio between the molecular mean free path and the characteristic length, falls in the range of $10^{-3} - 10^{-2}$ and the evaporation system can be considered in the continuum regime, where evaporation is controlled by diffusion and the coexisting phases can be assumed in equilibrium. The liquid–vapor phase equilibrium at the interface is described by the relation:

$$x_i P_s(T) = y_i P \tag{1}$$

where $P_s(T)$ is the saturated vapor pressure, P is the gas phase total pressure, x_i and y_i are the liquid and vapor mole fraction of the component (i).

The mass transport of an isotropic diffusing system is described by the equation of continuity of the species with concentration c:

$$\frac{\partial c}{\partial t} = D\nabla^2 c \tag{2}$$

This equation has been solved for the vapor phase considering a constant concentration in the liquid phase (due to the relatively small experiment time). Correlations for the vapor–liquid equilibrium and accurate models for the thermodynamic and transport properties have been considered from literature for reliable simulations.

Once the concentration field in the vapor phase is calculated, the concentration gradient in the liquid phase and the surface heat flux are evaluated and prescribed along the meniscus interface. In this way the temperature and velocity fields are computed in the liquid phase solving, with the finite volume algorithm based on the SIMPLE method by Patankar [23] available in the FLUENT/ANSYS commercial code, the governing equations:

$$\begin{aligned} &\nabla \cdot V = 0 \\ &\frac{\partial V}{\partial t} + V \cdot \nabla V + \frac{1}{\rho}\nabla p - \frac{1}{\rho}\mu\nabla^2 V = 0 \\ &\frac{\partial T}{\partial t} + V \cdot \nabla T = \alpha\nabla^2 T \end{aligned} \tag{3}$$

where V is the velocity vector, T the temperature, p the pressure, μ the viscosity, α the thermal diffusivity, t the time. The boundary conditions at the meniscus interface read:

$$\begin{aligned} &\dot{q} = JH_{LV} = \rho_V D H_{LV}\frac{\partial c}{\partial x} \\ &\tau = -\sigma_T \frac{\partial T}{\partial S} \end{aligned} \tag{4}$$

where the subscripts (V) denotes the vapor phase, (L) the liquid phase, $\dot{q}$ is the heat flux, D the diffusion coefficient, τ the viscous shear stress, σ_T is the surface tension derivative with temperature, S is the surface coordinate, H_{LV} is the latent heat of vaporization. The mass flux J across the meniscus is evaluated for the different mixtures.

The system under study is binary, so that solutal Marangoni convection, in addition to thermocapillary convection, could also be important. Analyses have been carried out to investigate if, on the surface of the meniscus, significant concentration gradients are established. The calculations accounted for the properties of the binary mixtures, in particular the diffusion coefficient of ethanol in water (10^{-9} m^2/s) considering the geometry under investigation and the interface evaporative mass flux distribution estimated according to the method discussed in Section 5. The simulations have been carried out in the two cases of purely diffusive evaporation and in presence of convection driven by surface tension, according to the experimental and numerical velocity fields discussed in Sections 3 and 6, respectively. Results show that, due to the relatively large solutal Peclet number (V^* ID/D_L, order of magnitude of 10^3) when convection was taken into account an almost uniform concentration distribution is established along the meniscus interface.

The main physical properties for ethanol, water and their mixtures, including density, heat capacity and thermal conductivity are shown in Table 1. The surface tension derivative and other properties, e.g. surface tension, viscosity, vapor pressure, etc., are correlated by polynomial regression from literature [20–22].

The meniscus shapes have been extracted from the experimental images for all tubes diameter and approximated by the analytical function given in Ref. [24]. In particular a contact angle equal to 57° has been obtained for all capillary tube diameters. The value is in good agreement with the measurement given in Ref. [25].

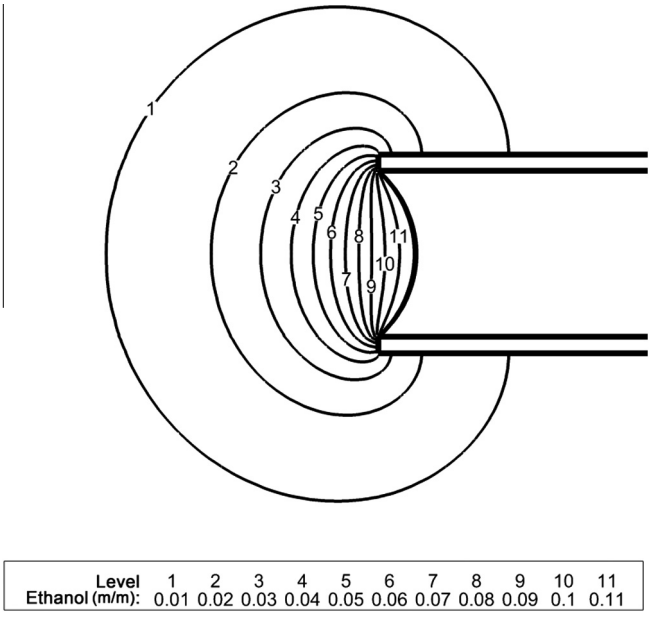

Fig. 5. Diffusion process shown by contours of the ethanol concentration in the vapor phase: ethanol vapor diffuses from the meniscus interface towards the surrounding ambient. Ethanol case, tube diameter equal to 1 mm.

Table 1
Fluid properties (T = 293 K, p = 1 atm).

Fluid	Ethanol	Ethanol 95% Water 5%	Ethanol 90% Water 10%	Ethanol 80% Water 20%
Liquid mole fraction x^*	1	0.88	0.78	0.61
Vapor mole fraction y^*	0.073	0.068	0.060	0.047
Density ρ (kg/m^3)	790	798	807	825
Specific heat C_P (J/kg/K)	2399	2474	2546	2713
Thermal conductivity K (W/m/K)	0.169	0.174	0.178	0.188

5. Alcohol diffusion, evaporation rate and heat/mass transfer

Heat and mass transfer from liquid vapor interface involves the evaporation of a volatile liquid from a fixed interface. In the proximity of meniscus, air is satured from the vapor that spontaneously flows away towards the ambient at lower concentration. As discussed by Dhavaleswarapu et al. [13], this continuously process is primarily dominated by Fick's law of binary diffusion which in turn depends on the surface properties of the sample liquid (contact angle, surface tension, etc.). As discussed in the previous paragraph, due to the presence of a meniscus, this gives a different evaporation rate along the liquid vapor interface winch in turn drives a Marangoni flow at the gas/liquid interface and two toroidal convection cells in the liquid phase.

Fig. 5 shows the numerical simulation results for the diffusion process (Eq. (2)) in the case of the evaporation of pure ethanol in air for 1 mm tube.

The mass flux, evaluated from the receding meniscus velocities, has been calculated according to the equation:

$$J = \rho_L V_M = \rho_V D \frac{\partial c}{\partial x} \tag{5}$$

where J is the mass flux, ρ_L the liquid densities, ρ_V the vapor densities, D the ethanol/air diffusion coefficient ($D = 1,\ 1 \times 10^{-5}$ m^2/s), c the local ethanol vapor concentration and V_M the receding velocity of the meniscus from experiments.

Differential evaporation rate along the meniscus gives a thermal gradient and therefore a thermocapillary flow directed from the center towards the capillary side. As explained above the heat flux was evaluated from the mass flux taking into account the latent heat of vaporization ($\dot{q} = JH_{LV} = \rho_V D H_{LV} \frac{\partial c}{\partial x}$). Fig. 6 shows the surface heat flux distribution due to the evaporation in the case of pure ethanol. Similar qualitative trends are found in the case of binary mixtures. Indeed the only major difference is the maximum heat flux that decreases with the evaporation rate when the water concentration increases.

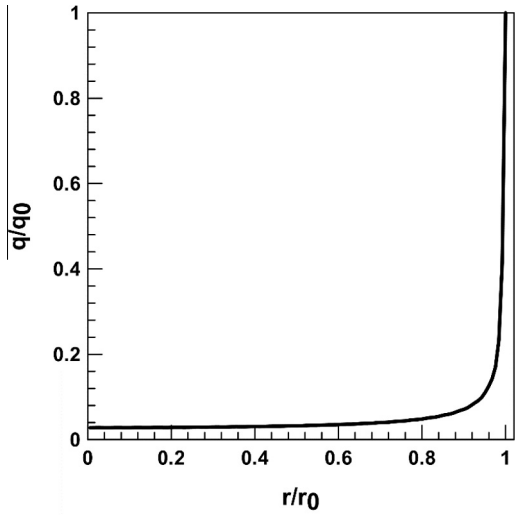

Fig. 6. Distribution of dimensionless heat flux along the meniscus. Heat flux and radial coordinate are normalized considering their maximum corresponding values.

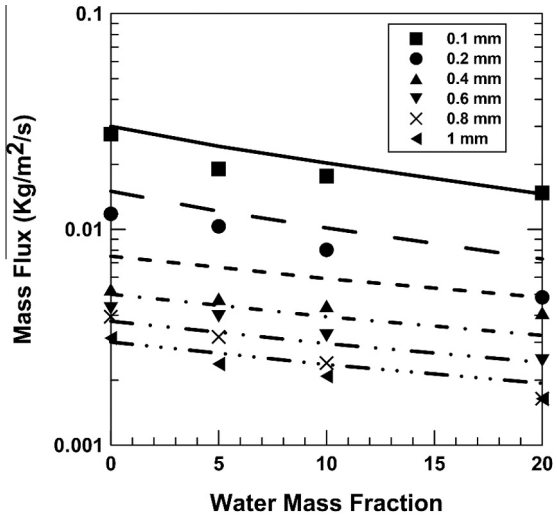

Fig. 7. Comparison between experimental and numerical average mass flux for different tube diameters. The points refer to the experimental measurements, the different lines show the numerical results.

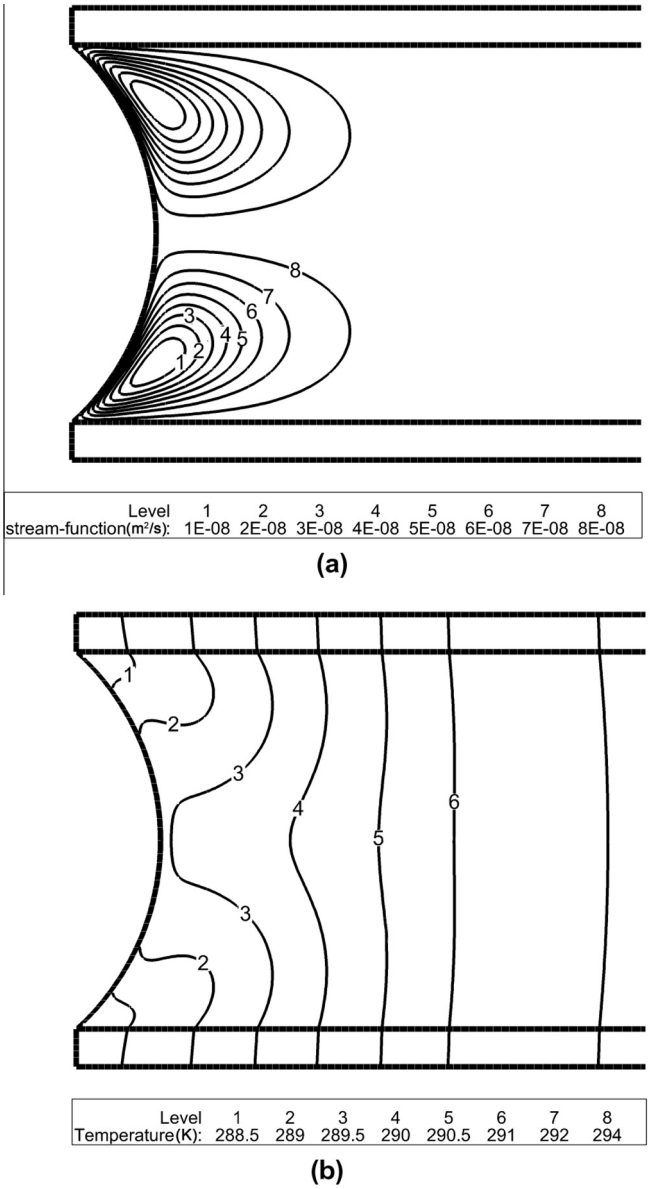

Fig. 8. Streamlines (a) and temperature distributions (b) in the liquid, for the case of pure ethanol and tube diameter equal to 1 mm. Stream function levels: (1) 10^{-8} m^2/s, (8) 8×10^{-8} m^2/s, delta = 10^{-8} m^2/s. Isotherms levels: (1) 288.5 K, (6) 291 K, delta = 0.5 K.

Fig. 7 shows a comparison between the measured and computed mass fluxes for ethanol and water/ethanol mixtures as a function of the water mass fraction in ethanol. The results are in agreement and show that the mass flux decreases with the tube diameter and with the water mass concentration.

6. Marangoni effect

The governing equations in the liquid phase (Eqs. (3) and (4)) have been discretized by the finite volume method using an axisymmetric model with a second order of upwind scheme. The SIMPLEC algorithm is used to couple the pressure and velocities variables. A convection heat transfer boundary condition (heat transfer coefficient, $h = 20\ W/m^2/K$) is imposed on to the external surface of the tube wall. The ambient temperature is fixed at 25 °C. Grid independence tests were performed for ethanol case using four sets of grid systems. It was found that minimum temperature and maximum velocities varied by less than 0.2% and 4%, respectively between the coarse (97×414) and fine grid system (193×639). A grid distribution of 97×414 grid point has been adopted for all the liquids investigated. An example of computed streamlines and temperature contours is shown in Fig. 8. Fig. 9 shows the surface distributions of heat flux and temperature (Fig. 9a) and the surface velocities (Fig. 9b) for different water concentrations in the case of a tube capillary with 1 mm inner diameter. It is evident that reducing the alcohol concentration the heat flux is smaller, due to the reduced evaporation rate, the surface temperature increases and the Marangoni velocities decrease.

Fig. 10 shows similar plots for the surface temperature, heat fluxes and velocities for different capillary diameters, in the case of pure ethanol. The Marangoni effect increases when the capillary size is reduced because, according to the plot of the surface heat flux (Fig. 10a), the concentration gradient at the liquid–vapor interface is higher for smaller tubes.

To evaluate the spinning frequency the tracer particles motion has been evaluated numerically using the Discrete Phase Model option available in FLUENT/ANSYS. Particle trajectories were obtained with Lagrangian approach. Newton's equation of motion of particle including inertia and friction factor is solved using a coupled approach where calculation of the continuum phase and discrete phase are alternated until a convergence coupled solution is achieved. No additional forces on particles have been considered

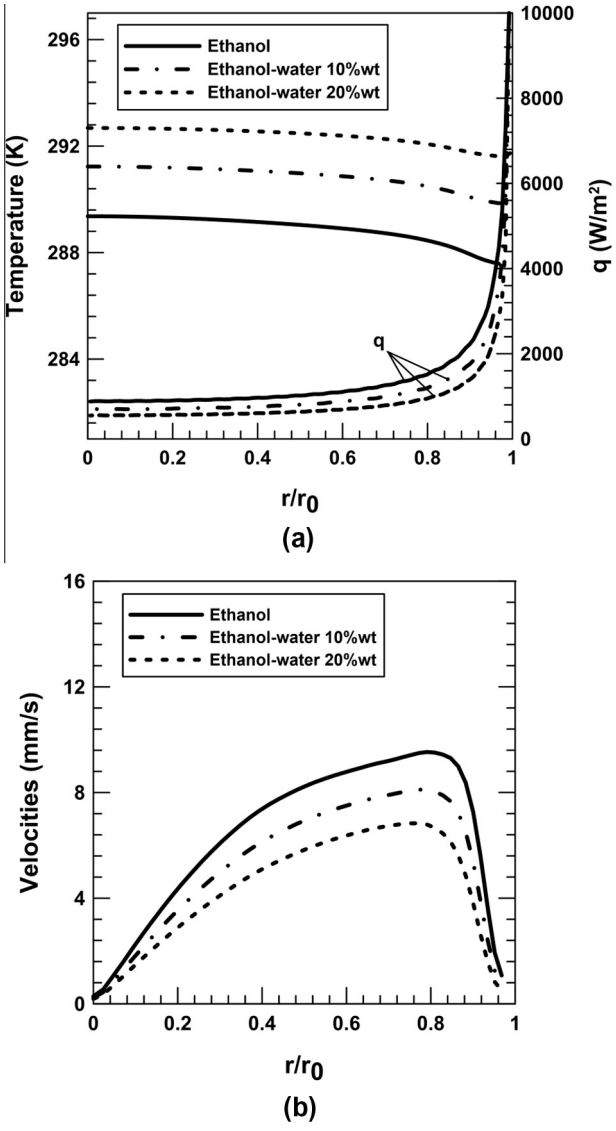

Fig. 9. Surface temperature and heat flux (a) and surface velocities (b) for different concentrations in the case of 1 mm tube.

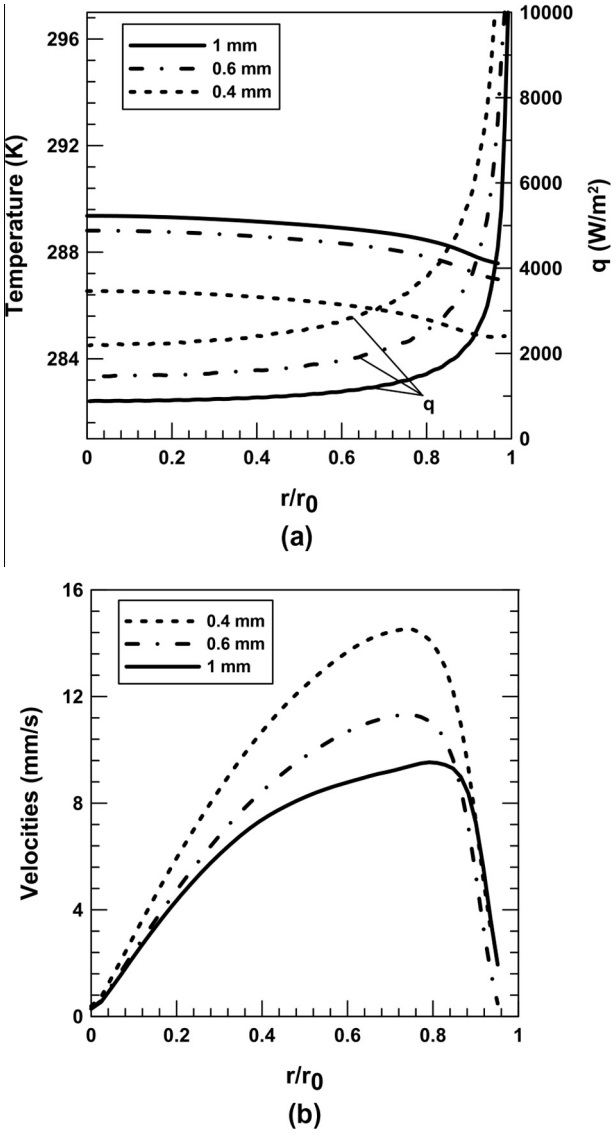

Fig. 10. Surface temperature and heat flux (a) and surface velocities (b) for different tube diameters in the case of pure ethanol.

Table 2
Comparison between numerical and experimental spinning frequencies (1/s).

Tube diameter	Water mass fraction					
	0		10%		20%	
	Experiment	Numerical	Experiment	Numerical	Experiment	Numerical
1 mm	2.03	2.17	1.58	1.81	1.27	1.41
0.8 mm	3.10	2.94	2.23	2.35	1.68	1.91
0.6 mm	4.28	4.17	2.95	3.34	2.30	2.71
0.4 mm	5.51	5.88	4.28	4.7	2.85	3.82

in the analysis. In general, considering several "numerical" tracer particles, they evolve and rapidly follow a closed Marangoni toroidal cell similar to the experiments. A typical particle path evolution has been shown in Fig. 2c.

A comparison between computed and measured spinning frequencies is shown in Table 2. The differences between computed and measured frequencies are in the order of 15%, which seem acceptable considering all possible numerical and experimental uncertainty. The maximum estimated error in locating the position of the spinning particle around a loop is +/−6%, which is determined by measuring the distance between the starting and ending position on one loop.

7. Conclusions

In the present work spontaneous Marangoni convection induced by evaporation of alcoholic solutions in cylindrical pipes from 100 to 1000 μm inner diameter has been presented and analyzed. The Marangoni toroidal convective flow has been characterized by measuring the spinning frequency and the average velocity of tracer particles; the evaporation rate has been measured and the evaporation flux derived. A numerical model has been developed that explains and correlates well the experimental results. The model solves the concentration field in the vapor phase surrounding the meniscus and the temperature and velocity fields in the liquid, based on the computed surface heat flux distribution. Very similar trends for the numerical and experimental results have been found for the different liquid solutions, in particular for the evaporation rate, the spinning frequency and the velocities for different tube diameter. In the case of binary mixtures the spinning frequency of the convective cells and the surface velocities are smaller when the alcohol concentration is reduced. This has been explained by the reduced driving force related to the lower evaporation rate.

Conflict of interest

None declared.

Acknowledgments

The authors wish to thank Miss C. Pulcrano for the efforts provided during the experiments performed at the Microgravity Research Centre in Bruxelles in the frame of the Erasmus Life Training Programme. We are also indebted with Prof. S. Van Vaerenbergh for financial support to the student mobility.

References

[1] D. Schwabe, Marangoni effects in crystal growth melts, Physicochem. Hydrodyn. 2 (4) (1981) 263–280.
[2] N. Ramanan, S.A. Korpela, Thermocapillary convection in an axisymmetric pool, Comput. Fluids 18 (2) (1990) 205–215.
[3] R. Savino, Surface tension-driven convection flow in evaporating liquid layers, in: Raffaele Savino (Ed.), Surface Tension-Driven Flows and Applications, Research Signpost, 2006, ISBN 81-308-0065-9.
[4] J.R.A. Pearson, On convection cells induced by surface tension, J. Fluid Mech. 4 (1958) 489–500.
[5] D. Reay, P. Kew, Heat Pipes: Theory, Design and Applications, fifth ed., Elsevier, London, 2006.
[6] P. Kavehpour, B. Ovryn, G.H. McKinley, Evaporatively-driven Marangoni instabilities of volatile liquid films spreading on thermally conductive substrates, Colloids Surf. A: Physicochem. Eng. Aspects 206 (1–3) (2002) 409–423.
[7] N. Zhang, P. Chao, Mechanism of convection instability in thin liquid layers induced by evaporation, Int. Commun. Heat Mass Transfer 26 (8) (1999) 1069–1080.
[8] D. Pratt, K.P. Hallinan, Thermocapillary effects on the wetting characteristics of a heated curved meniscus, J. Thermophys. Heat Transfer 11 (4) (1997) 519–525.
[9] D. Pratt, J. Brown, K.P. Hallinan, Thermocapillary effects on the stability of a heated, curved meniscus, J. Heat Transfer 120 (1) (1998) 220–226.
[10] C. Buffone, K. Sefiane, Investigation of thermocapillary convective patterns and their role in the enhancement of evaporation from pores, Int. J. Multiph. Flow 30 (2004) 1071–1091.
[11] C. Buffone, K. Sefiane, IR measurements of interfacial temperature during phase change in a confined environment, Exp. Thermal Fluid Sci. 29 (2004) 65–74.
[12] C. Buffone, K. Sefiane, J.R. Christy, Experimental investigation of self-induced thermocapillary convection for an evaporating meniscus in capillary tubes using micro-particle image velocimetry, Phys. Fluids 17 (2005) 052104.
[13] H.K. Dhavaleswarapu, P. Chamarthy, S.V. Garimella, J.Y. Murthy, Experimental investigation of steady buoyant thermocapillary convection near an evaporating meniscus, Phys. Fluids 19 (2007) 082103.
[14] P. Chamarthy, H.K. Dhavaleswarapu, S.V. Garimella, J.Y. Murthy, S.T. Wereley, Visualization of convection patterns near an evaporating meniscus using μPIV, Exp. Fluids 44 (2008) 431–438.
[15] Z. Pan, F. Wang, H. Wang, Instability of Marangoni toroidal convection in a microchannel and its relevance with the flowing direction, Microfluid. Nanofluid. 11 (2011) 327–338.
[16] C. Buffone, K. Sefiane, W. Easson, Marangoni-driven instabilities of an evaporating liquid–vapor interface, Phys. Rev. E 71 (2005).
[17] C. Minetti, C. Buffone, Three-dimensional Marangoni cell in self-induced evaporating cooling unveiled by digital holographic microscopy, Phys. Rev. E 89 (2014).
[18] J. Zhang, R.P. Behringer, A. Oron, Marangoni convection in binary mixtures, Phys. Rev. E 76 (2007) 016306.
[19] H. Wang, J.Y. Murthy, S.V. Garimella, Transport from a volatile meniscus inside an open microtube, Int. J. Heat Mass Transfer 51 (2008) 3007–3017.
[20] D. Mackay, W.Y. Shiu, K.-C. Ma, S.C. Lee, Handbook of physical–chemical properties and environmental fate for organic chemicals, in: Introduction and Hydrocarbons, Taylor and Francis, Boca Raton, FL, USA, 2006. vol. 1.
[21] I.S. Khattab, F. Bandarkar, M.A.A. Fakhree, A. Jouyban, Density, viscosity, and surface tension of water + ethanol mixtures from 293 to 323 K, Korean J. Chem. Eng. 29 (6) (2012) 812–817.
[22] E. Alvarez, J.M. Navaza, Surface tension of alcohol + water from 20 to 50 °C, J. Chem. Eng. Data 40 (3) (1995) 611–614.
[23] S.V. Patankar, Numerical Heat Transfer and Fluid Flow, Taylor & Francis, 1980. ISBN: 978-0891165224.
[24] B. Lan, Y.R. Li, D.F. Ruan, Numerical simulation of thermocapillary flow induced by non-uniform evaporation on the meniscus in capillary tubes, Microgravity Sci. Technol. 23 (1) (2011) S35–S42.
[25] K. Sefiane, M. Snodgrass, A. Steinchen, Evaporation self-induced Marangoni motion in fed capillaries for volatile liquids in open air, J. Non-Equilib. Thermodyn. 29 (2) (2004) 177–198.